Pharm Res (2011) 28:1282–1293
DOI 10.1007/s11095-011-0391-z

RESEARCH PAPER

Controlled Release of IGF-1 and HGF from a Biodegradable Polyurethane Scaffold

Devin M. Nelson • Priya R. Baraniak • Zuwei Ma • Jianjun Guan • N. Scott Mason • William R. Wagner

Received: 30 September 2010 / Accepted: 3 February 2011 / Published online: 23 February 2011

ABSTRACT

Purpose Biodegradable elastomers, which can possess favorable mechanical properties and degradation rates for soft tissue engineering applications, are more recently being explored as depots for biomolecule delivery. The objective of this study was to synthesize and process biodegradable, elastomeric poly (ester urethane)urea (PEUU) scaffolds and to characterize their ability to incorporate and release bioactive insulin-like growth factor–1 (IGF-1) and hepatocyte growth factor (HGF).

Methods Porous PEUU scaffolds made from either 5 or 8 wt% PEUU were prepared with direct growth-factor incorporation. Long-term *in vitro* IGF-1 release kinetics were investigated in saline or saline with 100 units/ml lipase to simulate *in vivo* degradation. Cellular assays were used to confirm released IGF-1 and HGF bioactivity.

Results IGF-1 release into saline occurred in a complex multiphasic manner for up to 440 days. Scaffolds generated from 5 wt% PEUU delivered protein faster than 8 wt% scaffolds. Lipase-accelerated scaffold degradation led to delivery of >90% protein over 9 weeks for both polymer concentrations. IGF-1 and HGF bioactivity in the first 3 weeks was confirmed.

Conclusions The capacity of a biodegradable elastomeric scaffold to provide long-term growth-factor delivery was demonstrated. Such a system might provide functional benefit in cardiovascular and other soft tissue engineering applications.

KEY WORDS elastomer · growth factor delivery · polyurethane · scaffold · tissue engineering

ABBREVIATIONS

BDI	1,4-diisocyanatobutane
bFGF	basic fibroblast growth factor
BSA	bovine serum albumin
DMEM	Dulbecco's modified Eagle medium
DMSO	dimethyl sulfoxide
HGF	hepatocyte growth factor
HUVECs	human umbilical vein endothelial cells

Devin M. Nelson and Priya R. Baraniak contributed equally to this work.

D. M. Nelson • P. R. Baraniak • W. R. Wagner
Department of Bioengineering, University of Pittsburgh
Pittsburgh, Pennsylvania, USA

D. M. Nelson • P. R. Baraniak • Z. Ma • J. Guan • W. R. Wagner
McGowan Institute for Regenerative Medicine
University of Pittsburgh
Pittsburgh, Pennsylvania, USA

N. S. Mason
Department of Radiology, University of Pittsburgh School of Medicine
Pittsburgh, Pennsylvania, USA

W. R. Wagner
Department of Chemical Engineering, University of Pittsburgh
Pittsburgh, Pennsylvania, USA

W. R. Wagner (✉)
McGowan Institute for Regenerative Medicine
450 Technology Drive, Suite 300
Pittsburgh, Pennsylvania 15219, USA
e-mail: wagnerwr@upmc.edu

Present Address:
P. R. Baraniak
The Wallace H. Coulter Department of Biomedical Engineering
Georgia Institute of Technology and Emory University
Atlanta, Georgia, USA

Present Address:
J. Guan
Department of Materials Science and Engineering
The Ohio State University
Columbus, Ohio, USA

IGF-1	insulin-like growth factor-1
MEM	minimum essential medium
PBS	phosphate-buffered saline
PCL	polycaprolactone
PEUU	poly(ester urethane)urea
TIPS	thermally induced phase separation

INTRODUCTION

The influence of substrate mechanical properties on cell proliferation, differentiation, and extracellular matrix production is increasingly appreciated (1,2). As such, more attention is being paid to the mechanical properties of candidate scaffolds for tissue engineering and regenerative medicine applications in an effort to improve functional outcomes. Historically, synthetic polymers used for cardiovascular replacement and repair have included non-degradable polymers such as poly(ethylene-terephthalate) and poly(tetrafluoroethylene), and tissue engineering approaches have frequently employed common polyesters such as poly(lactide), poly(glycolide), and their copolymers (3). However, these polymers are relatively stiff and not mechanically similar to native cardiovascular tissue. Polyurethanes as a class of polymers are attractive for soft tissue applications because of their ability to exhibit elastic behavior generally similar to many soft tissues and to be able to do so through physical crosslinking. To this end, biodegradable elastomeric polyurethanes have been developed using a variety of techniques to introduce lability (4–7), and these materials have been investigated in several locations *in vivo*, including both vascular and myocardial applications (8,9).

In order to enhance cellular infiltration into and survival within scaffolds and to direct the differentiation of endogenous and exogenous stem cell populations *in situ*, agents such as growth factors and adhesion molecules have been incorporated into polyurethane scaffolds for controlled release (10–15). The kinetics describing drug release from biomaterial scaffolds can be complex and varied. For example, many systems demonstrate simple diffusion-controlled delivery characterized by a burst release of near-surface drug, a subsequent fast diffusion period, and ending with lower release rates as the agent is exhausted (16). However, in the case of biodegradable materials, a two-stage release profile can also be observed, wherein a significant amount of drug remains trapped in the material bulk until adequate degradation of the material occurs, at which point the remaining drug diffuses out quickly (17). Other drug release profiles, including constant zero-order release or even triphasic release, can be achieved depending on factors such as material composition, material processing, drug physical properties, and drug loading (17,18). In the case of biomolecule delivery from polyurethane scaffolds, studies generally do not extend beyond a few weeks, meaning that the complexities of the release kinetics may be left unobserved. Additionally, whereas enzymes have been routinely used to investigate polyurethane degradation, reports of the use of enzymes in the context of controlled release are scarce (19,20).

Of particular interest for controlled release applications in myocardial tissue engineering is insulin-like growth factor-1 (IGF-1), which has been implicated in many physiological processes including tissue growth, protection and repair. Specifically, IGF-1 has been linked to several pathways in skeletal muscle formation and regeneration (21) and is expressed during the early and middle stages of muscle repair (22–24). Following myocardial infarction, IGF-1 has been shown to stimulate hypertrophy and prevent cardiomyocyte death, thereby attenuating ventricular dilation (25). Another growth factor that plays both a protective and reparative role in cardiac muscle is hepatocyte growth factor (HGF) (26–28). However, the therapeutic use of these growth factors is limited by their short half-lives *in vivo* (29,30). Thus, the sustained delivery of IGF-1 or HGF coupled with the attractive mechanical properties of a biodegradable elastomeric polyurethane scaffold may prove more advantageous for myocardial or skeletal muscle repair and regeneration than the administration of growth factor or polymer matrix alone.

The objective of the current study was to synthesize and process a biodegradable elastomeric poly(ester urethane) urea (PEUU) with the ability to incorporate and release bioactive IGF-1 and HGF. Porous PEUU scaffolds were fabricated using a thermally induced phase separation technique, and growth factors were directly incorporated into scaffolds during preparation. The long-term *in vitro* release kinetics of IGF-1 from scaffolds were investigated in phosphate-buffered saline (PBS) and in the presence of the enzyme lipase to simulate *in vivo* degradation. The bioactivity of released IGF-1 was confirmed with *in vitro* cell assays. HGF was also loaded into PEUU scaffolds, and while controlled release kinetics were not evaluated, it was also shown to maintain bioactivity upon release.

MATERIALS AND METHODS

Biodegradable Poly(ester urethane)urea (PEUU) Synthesis

PEUU based on polycaprolactone diol (PCL, MW = 2000, Aldrich), 1,4-diisocyanatobutane (BDI, Fluka), and putrescine (Aldrich) was synthesized in a two-step solution polymerization as previously reported (Fig. 1) (4). In brief, a 15 wt% solution of PCL in dimethyl sulfoxide (DMSO) was stirred with a 5 wt% solution of BDI in DMSO under argon gas. Stannous octoate, the catalyst, was added, and the reaction was allowed to continue at 80°C for 3 h with

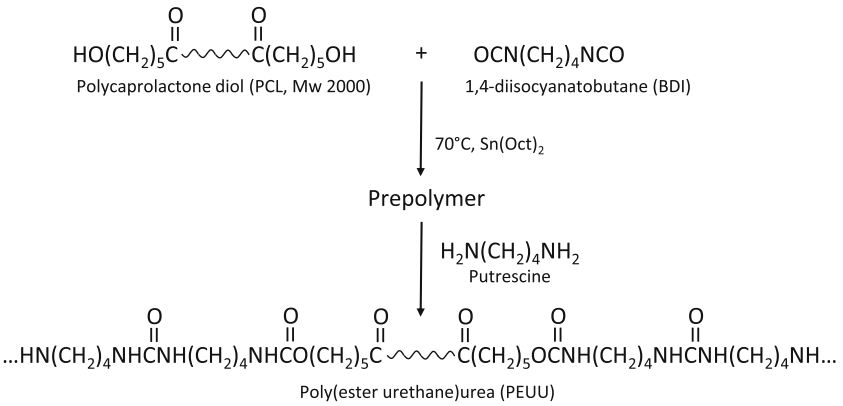

Fig. 1 Synthesis of PEUU. Poly (caprolactone) diol reacts with 1,4 diisocyanatobutane to form the prepolymer. The final product is formed by chain extension of prepolymer with putrescine.

constant stirring. After this time, the prepolymer solution was removed from heat and allowed to cool to room temperature. Putrescine in DMSO was then added dropwise, with constant stirring, to the prepolymer solution, and the reaction was allowed to continue at room temperature for 12–18 h. The stoichiometry of the reaction was 2:1:1 BDI:PCL:putrescine. The PEUU solution was precipitated in distilled water and immersed in isopropanol to remove unreacted monomers. Finally, the polymer was dried under vacuum at 50°C.

Fabrication of Three-Dimensional Growth-Factor-Loaded PEUU Scaffolds

Three-dimensional, porous PEUU scaffolds were fabricated by a thermally induced phase separation (TIPS) method (31). Following synthesis, PEUU was dissolved in DMSO at 80°C to make 5 or 8 wt% polymer solutions. Insoluble cross-linked polymer was removed by centrifugation at 250xg, and PEUU solution was once again heated to 80°C. Hot polymer solution was injected into a cylindrical glass mold (inner diameter 10 mm) capped with rubber stoppers. The mold was immediately placed at −80°C for 3 h. The cylinder end caps were then removed, and the mold was transferred to 200-proof ethanol for 3–7 days at 4°C for solvent extraction. Solvent extraction was considered complete once the polymer scaffold detached from the edges of the glass mold. Following DMSO removal, scaffolds were placed in water overnight to remove ethanol and reconstitute pore structure. Finally, the scaffolds were vacuum-dried for 24 h. Electron microscopy was used to verify porous scaffold morphology.

To fabricate growth-factor-loaded scaffolds, IGF-1 and HGF (R&D Systems) were first reconstituted in PBS in an excess of bovine serum albumin (BSA) (1:100, wt:wt) to stabilize the protein. Solutions containing growth factor and BSA were then snap-frozen in liquid nitrogen and vacuum-dried for 48 h. Dried proteins with salts were mixed with DMSO to make IGF-1 and HGF stock solutions at a concentration of 25 μg/ml. Growth factor in DMSO was added to the polymer solution at 80°C under rapid stirring for 15 s to make protein homogeneous in solution, after which the solution was injected into a cylindrical glass mold and immediately transferred to −80°C. ^{125}I-IGF-1 was synthesized following previously published methods (32). IGF-1 and ^{125}I-IGF-1-loaded scaffolds contained 2.5 mg of BSA and a final IGF-1 concentration of 500 ng/ml in PEUU solution. HGF-loaded scaffolds contained 2.5 mg of BSA and a final HGF concentration of 250 ng/ml in PEUU solution. Scaffolds were also fabricated without growth factor, but with BSA.

Mechanical Testing of PEUU Scaffolds

Scaffolds with and without growth factor were snap frozen in liquid nitrogen and cut into 500 μm-thick discs. In order to demonstrate similarity to scaffolds previously reported (15), tensile properties were measured on an MTS Tytron^{TM} 250 MicroForce Testing Workstation (10 mm/min crosshead speed) according to ASTM D638. Five samples were tested for each scaffold.

Degradation of PEUU Scaffolds

BSA-loaded scaffold disks were weighed and then immersed in PBS with or without 2 μl lipase enzyme solution (Sigma Aldich, 100 units/ml final concentration) at 37°C. At specified time points, scaffolds ($n=3$) were collected, dried, and weighed. After collecting the data for each time point, the studied scaffolds were discarded. The mass of dry scaffolds at each time point was compared to the starting dry mass of the sample. Release fluid was changed at regular intervals in order to maintain a constant pH and to keep an active concentration of enzyme present. Differential scanning calorimetry (DSC) of scaffold disks ($n=3$) at different stages of enzymatic degradation over 1 week, or without enzyme over 2 weeks, was completed using a Thermal Analyst 2000 (TA Instruments) DSC 2910

differential scanning calorimeter. Scaffold disks were heated from −100°C to 80°C at a heating rate of 10°C/min.

Quantification of Growth Factor Release from PEUU Scaffolds

Release kinetics for PEUU scaffolds containing ^{125}I-IGF-1 were determined *in vitro*. Scaffold disks (750 μm thickness, 10 mm diameter) were placed in test tubes and incubated in release media consisting of either 2 ml PBS or 2 ml PBS + 100 U/ml lipase enzyme per well at 37°C. Releasate was collected at pre-determined time points and replaced with 2 ml of fresh release media. The calculation of protein release at every time point was adjusted to account for the radioactive decay of I^{125} which is 59.6 days. These studies extended for up to a 440-day period. Growth-factor release was determined by quantifying the radioactivity of the release fluid using a gamma counter (Auto Gamma II, Perkin Elmer).

Verification of Bioactivity of Released Growth Factor

The bioactivity of IGF-1 released from scaffolds without lipase enzyme was measured by a cell mitogenicity assay employing Balb/3T3 cells (a mouse embryonic fibroblast cell line, R&D Systems) and MG-63 cells (a human osteosarcoma cell line, R&D Systems). These cell types were selected due to their documented dose-dependent proliferation in response to IGF-1 treatment (33,34). Preliminary studies involving direct addition of IGF-1 to these cells over a range from 0 to 200 ng/ml showed a maximum growth response for both cell types at 150 ng/mL IGF-1. Thus, this concentration was used as the standard for comparison in bioactivity assays. The bioactivity of released HGF was measured by a cell motogenic assay, and human umbilical vein endothelial cells (HUVECs) were selected due to their documented motogenic response to HGF (35). Scaffold disks (500 μm thickness, 10 mm diameter) with and without growth-factor loading were placed into wells of 24-well tissue culture plates in cell basal media (Minimum Essential Medium (MEM) for MG-63 cells and Dulbecco's Modified Eagle Medium (DMEM) for Balb/3T3 cells, both without fetal bovine serum). Basal medium from wells containing scaffolds was collected at pre-determined time points over 3 weeks, sterile-filtered, and kept frozen at −20°C until transfer to cells.

Balb/3 T3 and MG-63 cells were plated at 1×10^4 cells/cm^2 in each well of 24-well TCPS plates in cell growth medium (MEM or DMEM supplemented with 10% fetal bovine serum and penicillin and streptomyocin). Prior to growth media exchange with polymer releasate (basal medium), cells were treated overnight with 1 μl/ml colcemid (Sigma Aldrich) to synchronize cell cycle. Cells were then washed with PBS to remove traces of colcemid and fed with the appropriate polymer releasate. Four days following releasate treatment, cell numbers were indirectly quantified using a colorimetric assay for mitochondrial activity (MTT assay) (34). MTT results were qualitatively confirmed by visual cell inspection. Cell numbers for cells cultured in releasate were normalized to cells maintained in growth media.

HUVECs were plated at 1×10^4 cells/cm^2 in each well of 6-well TCPS plates in growth medium (endothelial basal medium, Lonza Inc). An *in vitro* wound healing assay was used to confirm the motogenic effect of HGF on cells (35). Briefly, once cells had grown to confluence, a cell scraper was used to create a wound down the center of each well of the 6-well plate. Cells were then washed with PBS to remove cell debris from the wound and treated with polymer releasate. A live-cell imaging system from Automated Cell Technology (ACT) was used to image cells at 10-min intervals over a 4-day period. Cell motility was quantified in terms of cell velocity (using ACT software) and cell migration into the wound (using NIH ImageJ software).

Statistical Analyses

Data are reported as mean ± standard deviation. All statistical analyses were performed using SPSS software. For cell proliferation, mass loss, and protein release studies, t-tests were used for evaluation of differences between two sets of data. For cell motility studies, mechanical properties, DSC data, and protein release data involving three or more data sets, data were analyzed by ANOVA with Tukey post-hoc testing for specific differences between various degradation solutions. Significance was defined as $p<0.05$.

RESULTS

Mechanical Properties of PEUU Scaffolds

TIPS scaffolds fabricated without the addition of any biomolecules (BSA or growth factors) had tensile strengths of 0.61±0.15 MPa. Scaffolds containing BSA alone had tensile strengths of 0.43±0.04 MPa, and scaffolds containing BSA and growth factor (IGF-1 or HGF) had tensile strengths of 0.32±0.18 MPa ($p>0.05$).

Degradation of PEUU Scaffolds

Scaffolds incubated in PBS did not demonstrate significant mass loss over the time period studied (Fig. 2). In the presence of lipase, scaffold, mass loss was substantially accelerated, with both polymer concentrations losing nearly half their mass over the first 2 days. With enzyme present,

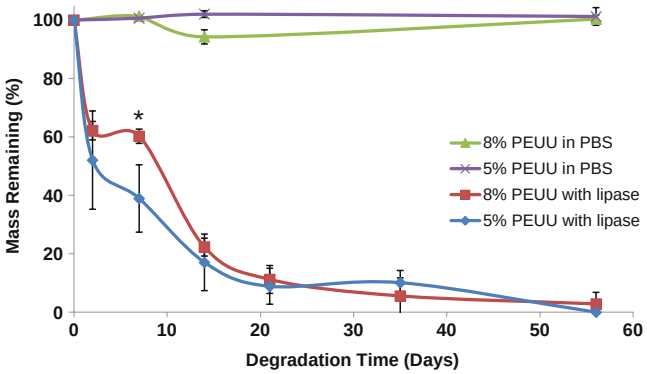

Fig. 2 The mass loss of PEUU scaffolds was determined over time for 5 and 8 wt% scaffolds soaked in PBS or with 100 units/ml lipase enzyme. * denotes $p < 0.05$ between scaffold polymer concentrations.

5 wt% scaffolds lost more mass over the first week compared to 8 wt% scaffolds with 38.9±11.5% and 60.2±2.5% mass remaining, respectively ($p<0.05$). Polymer degradation was nearly complete after 8 weeks. Morphologically, scaffolds maintained an organized pore structure, and after 1 week of incubation with lipase, the polymer surfaces were noticeably broken apart (Fig. 3).

DSC confirmed the degradation of scaffolds in the presence of enzyme. The melting temperature (T_m) for original scaffolds was around 50°C for both 5 wt% and 8 wt% scaffolds (Table 1 and Fig. 4). During degradation, a significantly lower second melting peak grew near 30°C as the primary peak weakened. By 7 days, the original peak was gone in 5 wt% scaffolds, though it continued to persist in 8 wt% scaffolds. Scaffolds in PBS did not show a significant change in T_m after 2 weeks.

IGF-1 Release from PEUU Scaffolds

Before samples were utilized in the release kinetics study, a substantial amount of IGF-1 had already been lost from the cylindrical scaffolds during DMSO extraction in ethanol. In particular, 8 wt% scaffolds lost 15% of loaded protein during this step compared to 50% for 5 wt% scaffolds. Thus, the starting mass of IGF-1 in 8 wt% and 5 wt%

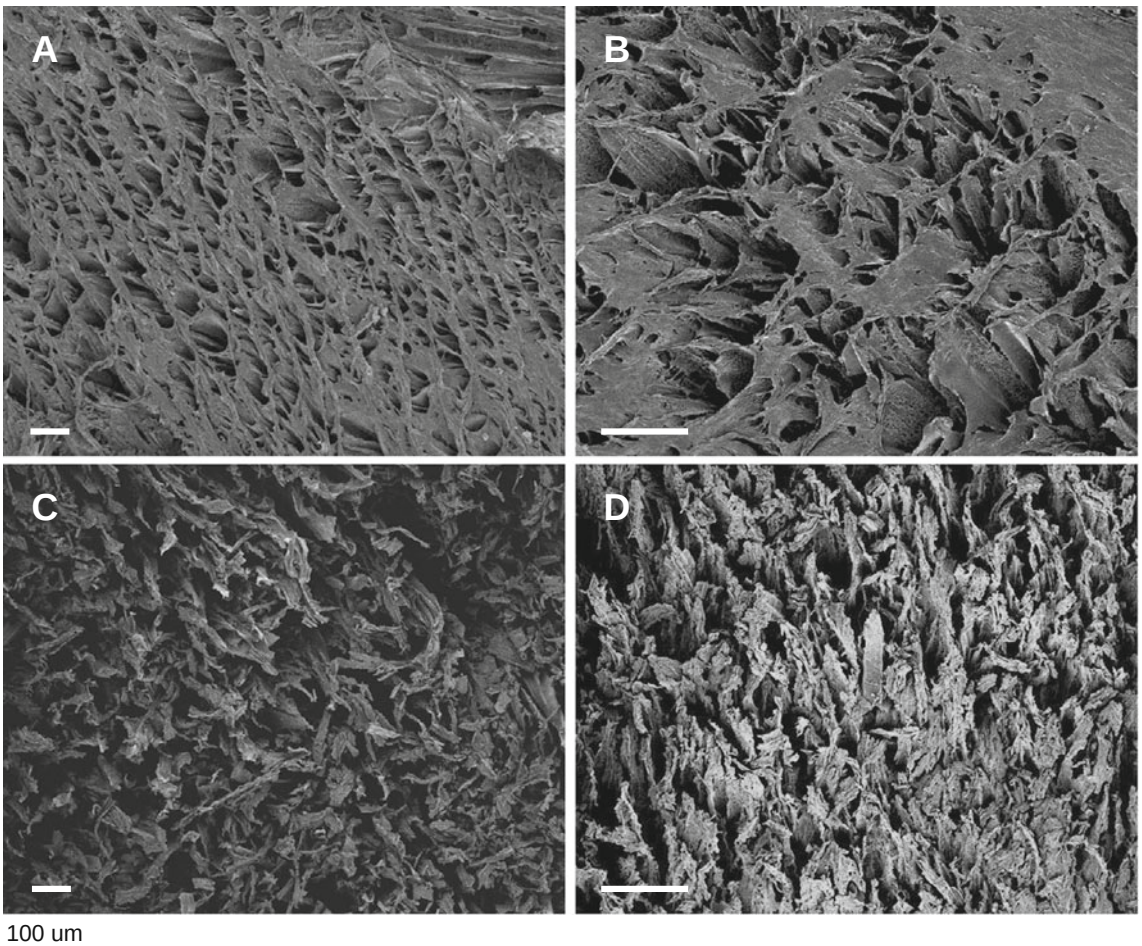

Fig. 3 Electron micrographs of TIPS scaffolds (5 wt% **A** and **C**, 8 wt% **B** and **D**) incubated in PBS (*top panels*) or lipase solution (*bottom panels*) for 1 week. Scaffolds maintained an organized pore structure after 1 week in PBS (*top panels*). After 1 week of incubation with lipase, scaffold surfaces were noticeably broken apart. Scale bar = 100 μm.

Table 1 Melting Temperature of Polymer Scaffolds

Scaffold wt%	Incubation conditions	Primary peak (°C)[a]	Secondary peak (°C)[a]
5 wt%	Original	51.0 ± 1.3	
	2 Days in Lipase	51.3 ± 0.2	36.2 ± 2.2*
	7 Days in Lipase	34.4 ± 4.6*	–
	14 Days in PBS	54.1 ± 0.8	–
8 wt%	Original	52.6 ± 1.3	–
	2 Days in Lipase	53.1 ± 0.7	36.3 ± 2.4*
	7 Days in Lipase	35.3 ± 3.1*	53.8 ± 0.02
	14 Days in PBS	54.8 ± 0.2	–

[a] data presented as mean ± standard deviation

*$p < 0.05$ compared to original Tm of same wt% scaffolds

scaffolds was 46.8 ± 7.5 and 22.5 ± 4.1 ng/scaffold, respectively. Once TIPS scaffold disks were immersed in PBS, the initial burst release occurred over 48 h, the extent of which was dependent on polymer concentration. Scaffolds with 8 wt% and 5 wt% polymer showed a burst release of 21.0 ± 1.0% and 10.3 ± 0.4%, respectively ($p < 0.001$) (Fig. 5a, Table 2). Following the burst release, there was an extended period of slow, steady protein release from scaffolds, termed latent phase I, and the release rate in this phase was faster in 5 wt% scaffolds (0.80%/week) than 8 wt% (0.39%/week) scaffolds ($p < 0.001$). Following latent phase I, a period of more rapid release occurred, labeled diffusion phase I, wherein 10–30% of protein was released. Observationally, the scaffolds showed distinct, moderate swelling at this point but maintained their shape. Upon handling, a qualitative reduction in modulus was noted. The initial burst, latent I, and diffusion I phases were followed by a second period of steady protein release (termed latent phase II) and then a second stage of accelerated protein release (termed

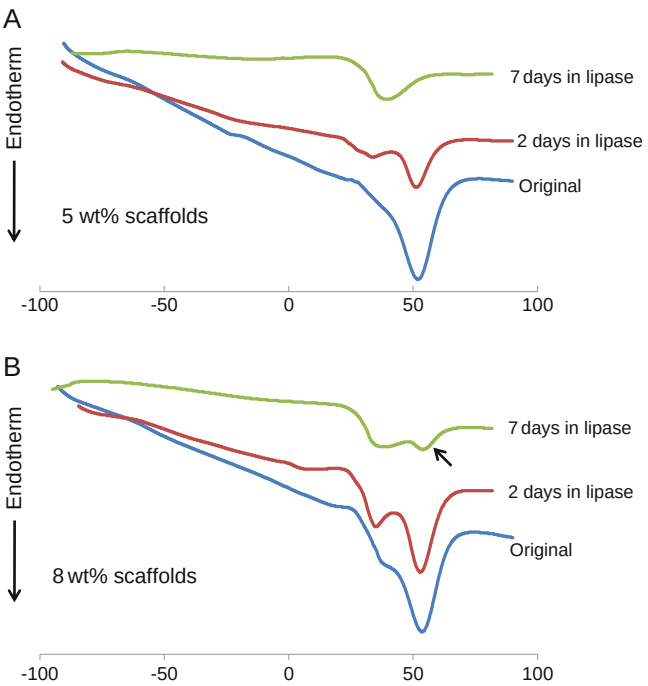

Fig. 4 DSC heating curves of 5 wt% (**A**) and 8 wt% (**B**) scaffolds during degradation with lipase enzyme. In all situations the initial primary melting temperature near 50°C is lost as a new substantial peak near 30°C is formed. Scaffolds with 8 wt% PEUU maintain the first peak for 7 days (black arrow), suggesting a slower degradation than 5 wt% scaffolds, which have lost that peak by 7 days.

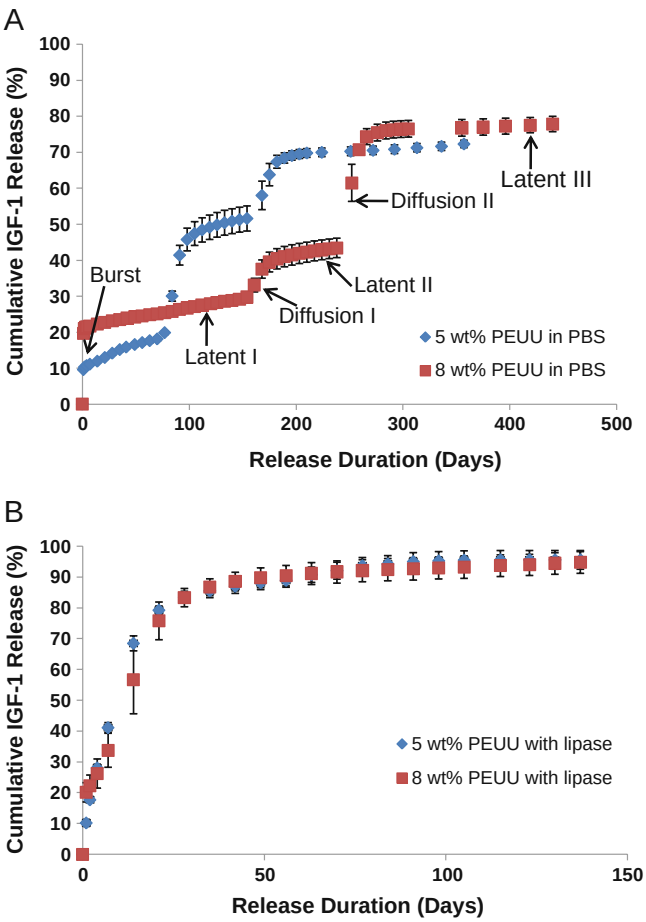

Fig. 5 (**A**) Scaffolds in PBS demonstrated a tri-phasic release profile for IGF-1 over the time period studied. Alternating periods of slow, steady protein release (*latent phases*) and more rapid release (*diffusion phases*) followed an initial burst release. (**B**) Both scaffold types incubated with 100 units/ml lipase enzyme released IGF-1 at a much faster rate than those without enzyme.

Table 2 IGF-1 Release Kinetics

Release phase	Phase begin (Day)	Phase end (Day)	Phase duration (Day)	Release Rate (%/week)[a]	Total IGF-1 Release (%)[a]
5 wt% PEUU scaffolds					
Burst	0	2	2	–	10.3 ± 0.41
Latent I	2	70	68	0.80 ± 0.04	7.8 ± 0.38
Diffusion I	70	112	42	–	30.3 ± 3.91
Latent II	112	154	42	0.53 ± 0.03	3.2 ± 0.16
Diffusion II	154	196	42	–	17.5 ± 2.89
Latent III	196	–	–	0.14 ± 0.02	–
8 wt% PEUU scaffolds					
Burst	0	2	2	–	21.0 ± 1.0
Latent I	2	147	145	0.39 ± 0.01	8.1 ± 0.22
Diffusion I	147	189	42	–	11.9 ± 2.10
Latent II	189	238	49	0.35 ± 0.02	2.4 ± 0.15
Diffusion II	238	284	46	–	32.6 ± 4.71
Latent III	284	–	–	0.08 ± 0.01	–

[a] data presented as mean ± standard deviation

diffusion phase II) from the scaffolds. Protein release after this point was very low for both polymer concentrations (latent phase III). Neither scaffold released all incorporated protein during the study, but radioactivity measurements confirmed that residual incorporated protein still resided within the polymer scaffolds, both types of which remained in a single piece throughout the study.

As is apparent in Fig. 5a and Table 2, the rate of protein release varied depending on the phase of the release profile and the initial polymer mass fraction. The rate of IGF-1 release decreased for each subsequent latency phase. For example, during latent phase I in 5 wt% scaffolds, IGF-1 released at 0.80%/week compared to 0.53%/week and 0.14%/week for the second and third latency periods, respectively ($p<.001$ between groups). The release rates in 8 wt% scaffolds followed a similar pattern but were consistently lower than for the 5 wt% scaffolds during these same latent phases at 0.39, 0.35, and 0.08%/wk respectively ($p<.001$ between groups). The 8 wt% scaffolds consistently demonstrated longer latent periods. For example, the latent phase I lasted over 20 weeks compared to 10 weeks for 5 wt% scaffolds. Interestingly, diffusion I and diffusion II phases lasted similar amounts of time for both scaffold mass fractions. The diffusion I stage released more protein in 5 wt% scaffolds than 8 wt% scaffolds (30.3 ± 3.9% *vs.* 11.9 ± 2.1%, $p<.001$) but the diffusion II stage release was the opposite with less release from 5 wt% scaffolds (17.5 ± 2.9% *vs.* 32.6 ± 4.7%, $p<.001$) than the 8 wt% counterparts.

Scaffolds incubated with lipase enzyme released protein much faster than those without enzyme, with more than 90% of IGF-1 being released after 9 weeks for both polymer concentrations (Fig. 5b). The distinct release phases observed with scaffolds in PBS were not apparent when enzyme was present. However, a noticeable attenuation of release rate was demonstrated in 8 wt% scaffolds compared to 5 wt% scaffolds during specific early time points. Specifically, IGF-1 release was slower in 8 *versus* 5 wt% scaffolds between days 1 and 2 (2.1 ± 0.8% *vs.* 7.5 ± 1.8%, respectively, $p<.05$), days 2–4 (4.0 ± 1.6% *vs.* 10.4 ± 0.5%, $p<.05$), and days 4–7 (7.6 ± 1.4%, *vs.* 13.1 ± 2.1%, $p<.05$).

Bioactivity of Released IGF–1 and HGF

MG-63 and Balb/3 T3 cells treated with releasate from IGF-1-containing scaffolds collected between days 0 and 7 and days 7 and 14 exhibited a significant increase in proliferation compared to those treated with degradation solutions from scaffolds without growth factor ($p<0.05$) (Fig. 6). Cellular proliferation was comparable to that for cells treated with 150 ng/ml IGF-1. Specifically, cells treated with day 0–7 releasate from scaffolds containing IGF-1 exhibited a 2.0-fold (MG-63) and 2.1-fold (Balb/3T3) increase in cell number compared to cells treated with releasate from scaffolds without growth factor. Cells treated with day 7–14 releasate from scaffolds containing IGF-1 exhibited a 1.6-fold (MG-63) and 1.7-fold (Balb/3T3) increase over cells in releasate from scaffolds without growth factor. No significant difference in cell proliferation was seen between cells treated with releasate collected between days 14–21 from either set of scaffolds. For HGF, following treatment with the day 0–7 and day 14–21 polymer releasate from scaffolds containing HGF, endothelial cells grew into and repopulated the wound area more extensively than those maintained in growth medium or in releasate from scaffolds without growth factor ($p<0.05$) (Fig. 7). Day 7–14 releasate was not collected to evaluate.

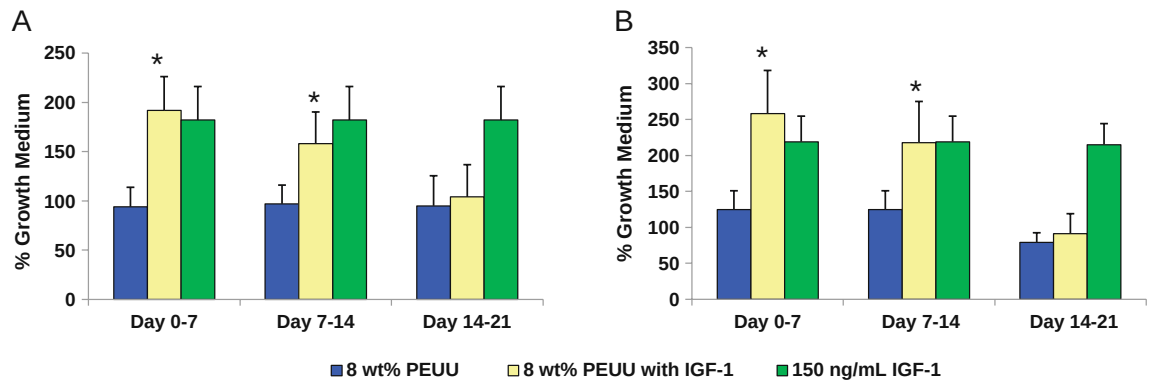

Fig. 6 MG-63 (**A**) and Balb/3T3 (**B**) cells cultured in releasate from polymer containing IGF-1 demonstrated significantly greater cell metabolic activity (as an index of cell number) compared to cells cultured in releasate from polymer without growth factor (*$p < 0.05$). IGF-1 added at 150 ng/ml to releasate from polymer without growth factor served as a positive control.

DISCUSSION

The release profiles of drugs from biodegradable elastomers vary widely depending on material composition and processing. Biodegradable thermoset elastomers based on ε-caprolactone and D,L-lactide have been processed with solid drug particles to form an osmotically driven drug delivery device that delivers drug in a zero-order fashion (18,36,37). The release rates in this system can be altered by changing the molecular weight of the prepolymer or the amount of excipient included with the drug. In another report, ascorbic acid was incorporated into the backbone of a thermoplastic polyurethane and released only after hydrolysis of ester bonds (14). This led to a slow release rate initially which increased substantially over time in a way that corresponded with bulk polymer degradation.

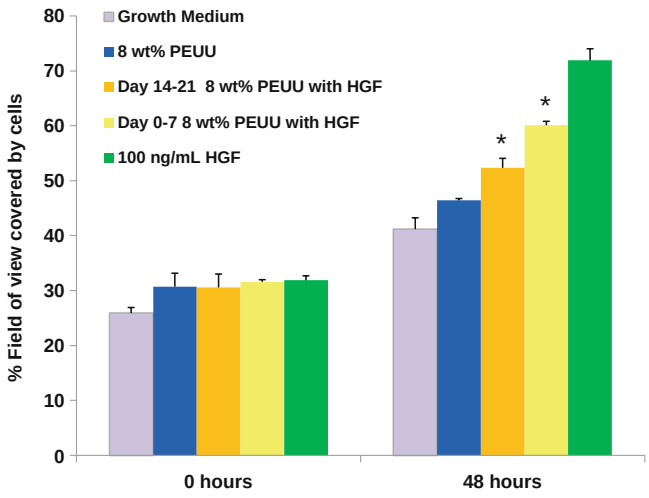

Fig. 7 HUVECs maintained in releasate from scaffolds containing HGF grew into and repopulated the artificial wound area more extensively than those maintained in growth medium or in releasate from scaffolds without growth factor (*$p < 0.05$). HGF added at 100 ng/ml to releasate from polymer without growth factor served as a positive control.

Many other biodegradable elastomers release molecules in a diffusion-controlled manner characterized by high initial release rates that quickly taper off (11,16,38). One such group, a family of injectable biodegradable polyurethanes, has been of particular interest due to their ability to crosslink *in situ* to form porous polymer scaffolds in a way that does not substantially decrease the bioactivity of incorporated drugs. These systems generally show a high initial release that plateaus after a few days, with 50–90% of drug being released depending on the drug loading mechanism and type of drug being delivered (10,39). Despite the fact that some members of this family are relatively slowly degrading (~30% mass loss over 36 weeks), release studies do not extend beyond a few weeks. This prevents understanding the mechanisms involved over time in a slow-degrading polyurethane and how the remaining 10–50% of protein is released from the system. In studying the long-term release kinetics of protein from PEUU, as has been done here, more insight may be gained toward developing extended release approaches for polyurethane systems.

IGF-1 release from this biodegradable porous scaffold system demonstrated a multi-phasic release profile. There are a number of drug delivery systems that follow a biphasic drug release profile characterized by two separate stages of quick drug release separated by a latency phase (17,40,41). The first phase of quick drug delivery occurs as drug is released that is either close to the surface or can easily diffuse out of the bulk of the material. Following this, delivery is slow in the latency phase until material degradation becomes adequate to loosen the scaffold and allow trapped drug to quickly diffuse out. The current report demonstrates a release profile wherein there are three distinct occurrences of rapid, diffusion-controlled release. Importantly, because the quantitative studies of IGF-1 release used radiolabeled protein, the release kinetics observed may be different from what actually occurs when

non-labeled IGF-1 is released, as in the case of the bioactivity studies. As the scaffolds for both studies were made with identical protocols and loading concentrations, the protein released at each stage would likely be similar. However, variation may arise due to potential differences between IGF-1 and ^{125}I-IGF-1 and processing variability.

While the exact mechanisms of the complex release profile are not clear and warrant further investigation, it is likely that the phase-segregated nature of PEUU plays a role. First, both hard and soft segments may act independently in relation to degradation and drug release. Additionally, PCL is known to contribute significant crystallinity to polyurethanes, the gradual breakdown of which can be delayed even in the presence of enzyme (5,42). It is possible that degradation follows a multi-step process where amorphous soft-segment, crystalline soft-segment, and hard-segment degradation occur separately with each stage influencing drug delivery. This hypothesis is supported by the DSC data which show a change in T_m during degradation. The transition from a T_m near 50°C to one near 30°C in the presence of lipase shows that the crystal structure of the polymer is being altered, particularly to a T_m below body temperature. In the case of the lower T_m, crystal structures would largely be melted above 37°C, which could loosen the polymer network and allow more protein to be released. It may be that one of the diffusion phases seen for protein release from scaffolds in PBS is the result of a transition from the higher T_m to the lower one. Additionally, the delayed loss of the initial melting peak for 8 wt% scaffolds agrees well with the slower mass loss and slower protein release that was demonstrated during enzymatic degradation of 8 wt% scaffolds compared to 5 wt%.

The differences in protein release between 5 wt% and 8 wt% scaffolds illustrate the influence that polymer mass fraction had on drug release. First, 5 wt% scaffolds lost more protein in the solvent extraction step of scaffold processing, meaning these scaffolds had a lower loading efficiency. Second, the delivery rates of protein from 5 wt% scaffolds were consistently higher and occurred at earlier time points than for 8 wt% scaffolds. This phenomenon may be attributed to the smaller mass fraction of PEUU in the 5 wt% scaffold disks, which led to more free volume for molecular diffusion out of the scaffold and less material that required degradation. Both polymer mass fractions, however, exhibited slower release rates for IGF-1 than had been shown previously when basic fibroblast growth factor (bFGF) was released from similar scaffolds (15). The reason for this difference is not clear but may be related to differences in the affinity of IGF-1 and bFGF to the polymer or the slower polymer degradation that was present here compared to the previous study. While no significant mass loss was seen in the scaffolds in PBS over the time period studied, in the presence of enzyme, scaffolds with 8 wt% polymer had attenuated mass loss, particularly in the first week compared to those with 5 wt% polymer. This difference in enzymatic degradation between 5 and 8 wt% scaffolds was noticeable in the release profiles where the rate of IGF-1 release was significantly lower between days 1 and 7 for the 8 wt% scaffolds.

The biodegradation of polyurethanes is a complex process that has gained significant attention in recent decades (43). Hydrolytically labile bonds in the soft segment provide the most common mechanism of degradation. It has been shown that both oxidative and enzymatic processes encouraged by inflammatory cells may speed polymer breakdown *in vivo* (44,45). Two common esterase enzymes produced by macrophages that have been utilized *in vitro* to simulate *in vivo* soft-segment biodegradation mechanisms are cholesterol esterase and lipase (20,42,44–46). The ability of cells and enzymes to degrade polyurethanes is dependent on many factors including hard- and soft-segment chemical composition, size, surface morphology and mechanical environment (45,47–49). These studies illustrate that numerous complex processes are involved in biomaterial degradation, which cannot be fully replicated *in vitro*.

The enzyme concentration in this report was chosen for its ability to provide a degradation rate that corresponded to scaffold breakdown over approximately 8 weeks, similar to what is histologically observed *in vivo* when a similar scaffold disk was implanted as a cardiac patch (8). The release profile exhibited when scaffolds were incubated with lipase demonstrated that for *in vivo* environments where material degradation was accelerated, release rates were markedly different than in the PBS environments often used for *in vitro* controlled release studies. The rapid rate of polymer degradation in the presence of enzyme made for protein release kinetics that appeared more like the simple diffusion-controlled systems discussed earlier, which was substantially different from the multiple phasic release profile seen in the PBS. Therefore, these data emphasize that researchers should consider the working environment when characterizing controlled release from biodegradable matrices, a practice not regularly seen in the literature.

Linear thermoplastic elastomers have an advantage over thermoset elastomers in that drugs can be readily incorporated during processing and in a way that does not risk drug inactivation during polymer crosslinking. In the current research, protein bioactivity was studied over the first 3 weeks of drug delivery. It is unclear if the loss of measurable cellular response to IGF-1 between day 14 and 21 was from a loss of bioactivity or simply due to the low protein release during that time period as seen in the release profile. The latter case would suggest that released protein was of insufficient concentration to influence cell behavior in the assay used, which might be corrected with a higher initial loading dose of protein. Additionally, it has

been shown that growth factors incorporated into thermoset degradable elastomers can maintain bioactivity over at least 3 weeks (36), suggesting that longer-term maintenance of bioactivity is feasible.

One limitation of the current research deals with understanding the maintenance of protein bioactivity during scaffold processing and throughout the release duration. To determine changes in bioactivity, the amount of protein released from a scaffold needs to be quantified, and then the functionality of that protein would be tested. However, in this report, two distinct experiments were employed to study IGF-1 release—quantitative release kinetics using radiolabeled protein and bioactivity of non-labeled released protein. Both were needed due to an inability to quantify non-labeled IGF-1 using enzyme-linked immunosorbent assays (ELISA) and other spectrophotometric techniques. The inability to detect both IGF-1 and HGF protein with these techniques may be related to the presence of polymer degradation products or conformational changes to the protein which would prevent binding of the monoclonal antibody in the ELISA sandwich assay. In particular, the TIPS processing involved mixing protein in organic solvent and brief exposure to high temperatures—both factors that could damage the loaded protein. In order to preserve bioactivity, BSA was added in excess to protect the protein of interest, as has been done previously (50). Importantly, in spite of any presumed destruction of protein or changes to protein binding in the ELISA, enough protein remained bioactive over the three week period studied to elicit the expected results on cell behavior *in vitro*.

One basis of controlled release formulations is that while proteins generally have a short half-life *in vivo*, their sequestration in a polymeric scaffold can act to protect them *in vivo* to prevent rapid degradation. An important finding in this research is that maintaining protein bioactivity for long durations as would be necessary for *in vitro* release studies may be irrelevant given the much faster release seen in conditions that mimic the *in vivo* environment. In the experiments using lipase, protein delivery was nearly complete after only 9 weeks compared to nearly 15 months for studies without lipase.

The ideal duration of IGF-1 delivery that would be desired is dependent on the drug delivery application. For example, in the case of cardiac ischemia, rapid delivery of IGF-1 in the days following injury has been shown to rescue injured myocardium (51). However, in the case of slowly progressing, chronic degenerative diseases such as inherited cerebellar ataxia (52) or diabetes (53), therapeutic options to treat severely debilitating symptoms are currently limited by the short *in vivo* life span of peptide molecules and the need to administer drugs to patients on a daily basis. In such cases, controlled-release formulations leading to sustained improvements in patient symptoms and/or disease conditions allow for more convenient dosage and increased compliance with treatment.

Scaffold processing was also noteworthy for its role in determining protein loading efficiency in PEUU scaffolds. The final step of scaffold synthesis using TIPS involved DMSO solvent extraction. This step required 3–7 days of soaking in ethanol, during which time a substantial amount of protein was lost to the solvent. While this method was necessary to create the mechanically robust, porous scaffolds studied here, other techniques such as salt-leaching may be considered which do not have a lengthy liquid-phase solvent extraction step. The short duration required to remove salts from thin scaffold disks in water (<20 min) may lead to less protein loss in solution initially, even in spite of the higher solubility of protein in water compared to ethanol. Regardless of processing technique, it is important to have a uniform distribution of protein throughout the scaffold. In this report, disks cut from locations throughout the initial cylindrical scaffold were used in the release experiments. The narrow standard deviation in the protein release kinetics among all disks suggests a homogeneous distribution of protein throughout the cylindrical scaffolds.

Tissue engineering often seeks to combine appropriate scaffolding materials with important signaling molecules to encourage healthy tissue regeneration. It has been demonstrated that the controlled delivery of IGF-1 and HGF from biomaterials in the context of ischemic myocardium has been influential in cardiac repair (51,54). These studies, however, utilize biomaterials that provide minimal mechanical support in a setting where such support may be advantageous. A mechanically robust, elastomeric scaffold similar to the one studied here was able to prevent further cardiac deterioration after its application as a surface patch following myocardial infarction (8). Combining the benefit of this temporary mechanical support system with growth-factor delivery might act to abrogate disease progression and encourage functional tissue repair in injured myocardium more effectively than either system independently.

CONCLUSION

A biodegradable elastomeric PEUU scaffold system was characterized for its ability to be loaded with and deliver growth factors (IGF-1 and HGF) of clinical relevance. Cellular assays confirmed that the bioactivity of IGF-1 and HGF was maintained during scaffold processing and for at least the early period of drug delivery. The kinetics of IGF-1 release over a period up to 440 days demonstrated a complex triphasic profile. Much of this complexity was lost and replaced by a single phase release profile when enzyme was present to simulate *in vivo* scaffold degradation. The

ease of processing associated with this thermoplastic biodegradable elastomer for both scaffold formation and drug loading makes this material an attractive option for soft tissue applications where both drug delivery and appropriate mechanical support are desired.

ACKNOWLEDGMENTS

This work was supported by the National Institutes of Health (NIH) grant #HL069368. Dr. Baraniak and Mr. Nelson were supported by NIH training grants #T32-EB001026-01 and #T32-HL076124, respectively.

REFERENCES

1. Rehfeldt F, Engler AJ, Eckhardt A, Ahmed F, Discher DE. Cell responses to the mechanochemical microenvironment–implications for regenerative medicine and drug delivery. Adv Drug Deliv Rev. 2007;59:1329–39.
2. Wells RG. The role of matrix stiffness in regulating cell behavior. Hepatology. 2008;47:1394–400.
3. Ramaswami P, Wagner WR. Cardiovascular tissue engineering. In: Guelcher S, Hollinger JO, editors. An Introduction to biomaterials. Boca Raton: CRC; 2006. p. 461–84.
4. Guan J, Sacks MS, Beckman EJ, Wagner WR. Synthesis, characterization, and cytocompatibility of elastomeric, biodegradable poly(ester-urethane)ureas based on poly(caprolactone) and putrescine. J Biomed Mater Res. 2002;61:493–503.
5. Skarja GA, Woodhouse KA. *In vitro* degradation and erosion of degradable, segmented polyurethanes containing an amino acid-based chain extender. J Biomater Sci Polym Ed. 2001;12:851–73.
6. Guan J, Wagner WR. Synthesis, characterization and cytocompatibility of polyurethaneurea elastomers with designed elastase sensitivity. Biomacromolecules. 2005;6:2833–42.
7. Gogolewski S, Galletti G. Degradable, microporous vascular prosthesis from segmented polyurethane. Colloid Polym Sci. 1986;264:854–8.
8. Fujimoto KL, Tobita K, Merryman WD, Guan J, Momoi N, Stolz DB, *et al.* An elastic, biodegradable cardiac patch induces contractile smooth muscle and improves cardiac remodeling and function in subacute myocardial infarction. J Am Coll Cardiol. 2007;49:2292–300.
9. He W, Nieponice A, Soletti L, Hong Y, Gharaibeh B, Crisan M, *et al.* Pericyte-based human tissue engineered vascular grafts. Biomaterials. 2010;31:8235–44.
10. Hafeman A, Li B, Yoshii T, Zienkiewicz K, Davidson J, Guelcher S. Injectable biodegradable polyurethane scaffolds with release of platelet-derived growth factor for tissue repair and regeneration. Pharm Res. 2008;25:2387–99.
11. Hafeman AE, Zienkiewicz KJ, Carney E, Litzner B, Stratton C, Wenke JC, *et al.* Local delivery of tobramycin from injectable biodegradable polyurethane scaffolds. J Biomater Sci Polym Ed. 2010;21:95–112.
12. Sivak WN, Zhang J, Petoud S, Beckman EJ. Incorporation of ionic ligands accelerates drug release from LDI-glycerol polyurethanes. Acta Biomater. 2010;6:144–53.
13. Stankus JJ, Freytes DO, Badylak SF, Wagner WR. Hybrid nanofibrous scaffolds from electrospinning of a synthetic biodegradable elastomer and urinary bladder matrix. J Biomater Sci Polym Ed. 2008;19:635–52.
14. Zhang J, Doll BA, Beckman EJ, Hollinger JO. A biodegradable polyurethane-ascorbic acid scaffold for bone tissue engineering. J Biomed Mater Res A. 2003;67A:389–400.
15. Guan J, Stankus JJ, Wagner WR. Biodegradable elastomeric scaffolds with basic fibroblast growth factor release. J Control Release. 2007;120:70–8.
16. Li B, Brown KV, Wenke JC, Guelcher SA. Sustained release of vancomycin from polyurethane scaffolds inhibits infection of bone wounds in a rat femoral segmental defect model. J Control Release. 2010;145:221–30.
17. Lao LL, Venkatraman SS, Peppas NA. A novel model and experimental analysis of hydrophilic and hydrophobic agent release from biodegradable polymers. J Biomed Mater Res A. 2009;90:1054–65.
18. Amsden B. A model for osmotic pressure driven release from cylindrical rubbery polymer matrices. J Control Release. 2003;93:249–58.
19. Amsden BG. Biodegradable elastomers in drug delivery. Expert Opin Drug Deliv. 2008;5:175–87.
20. Woo GLY, Yang ML, Yin HQ, Jaffer F, Mittelman MW, Santerre JP. Biological characterization of a novel biodegradable antimicrobial polymer synthesized with fluoroquinolones. J Biomed Mater Res. 2002;59:35–45.
21. Rosenthal N, Musaro A. Gene therapy for cardiac cachexia? Int J Cardiol. 2002;85:185–91.
22. Schulze PC, Fang J, Kassik KA, Gannon J, Cupesi M, MacGillivray C, *et al.* Transgenic overexpression of locally acting insulin-like growth factor-1 inhibits ubiquitin-mediated muscle atrophy in chronic left-ventricular dysfunction. Circ Res. 2005;97:418–26.
23. Hayashi S, Aso H, Watanabe K, Nara H, Rose MT, Ohwada S, *et al.* Sequence of IGF-I, IGF-II, and HGF expression in regenerating skeletal muscle. Histochem Cell Biol. 2004;122:427–34.
24. Machida S, Booth FW. Insulin-like growth factor 1 and muscle growth: implication for satellite cell proliferation. Proc Nutr Soc. 2004;63:337–40.
25. Padin-Iruegas ME, Misao Y, Davis ME, Segers VF, Esposito G, Tokunou T, *et al.* Cardiac progenitor cells and biotinylated insulin-like growth factor-1 nanofibers improve endogenous and exogenous myocardial regeneration after infarction. Circulation. 2009;120:876–87.
26. Jin H, Wyss JM, Yang R, Schwall R. The therapeutic potential of hepatocyte growth factor for myocardial infarction and heart failure. Curr Pharm Des. 2004;10:2525–33.
27. Duan HF, Wu CT, Wu DL, Lu Y, Liu HJ, Ha XQ, *et al.* Treatment of myocardial ischemia with bone marrow-derived mesenchymal stem cells overexpressing hepatocyte growth factor. Mol Ther. 2003;8:467–74.
28. Ueda H, Nakamura T, Matsumoto K, Sawa Y, Matsuda H. A potential cardioprotective role of hepatocyte growth factor in myocardial infarction in rats. Cardiovasc Res. 2001;51:41–50.
29. Pulavendran S, Rajam M, Rose C, Mandal AB. Hepatocyte growth factor incorporated chitosan nanoparticles differentiate murine bone marrow mesenchymal stem cell into hepatocytes *in vitro*. IET Nanobiotechnol. 2010;4:51.
30. Kato N, Nakanishi K, Nemoto K. Efficacy of HGF gene transfer for various nervous injuries and disorders. Cent Nerv Syst Agents Med Chem. 2009;9:300–6.
31. Guan J, Fujimoto KL, Sacks MS, Wagner WR. Preparation and characterization of highly porous, biodegradable polyurethane scaffolds for soft tissue applications. Biomaterials. 2005;26:3961–71.
32. Kricker JA, Towne CL, Firth SM, Herington AC, Upton Z. Structural and functional evidence for the interaction of insulin-like growth factors (IGFs) and IGF binding proteins with vitronectin. Endocrinology. 2003;144:2807–15.

33. Liu XJ, Xie Q, Zhu YF, Chen C, Ling N. Identification of a nonpeptide ligand that releases bioactive insulin-like growth factor-I from its binding protein complex. J Biol Chem. 2001;276:32419–22.
34. Singh M, Shirley B, Bajwa K, Samara E, Hora M, O'Hagan D. Controlled release of recombinant insulin-like growth factor from a novel formulation of polylactide-co-glycolide microparticles. J Control Release. 2001;70:21–8.
35. Bussolino F, Di Renzo MF, Ziche M, Bocchietto E, Olivero M, Naldini L, *et al.* Hepatocyte growth factor is a potent angiogenic factor which stimulates endothelial cell motility and growth. J Cell Biol. 1992;119:629–41.
36. Gu F, Neufeld R, Amsden B. Sustained release of bioactive therapeutic proteins from a biodegradable elastomeric device. J Control Release. 2007;117:80–9.
37. Gu F, Neufeld R, Amsden B. Osmotic-driven release kinetics of bioactive therapeutic proteins from a biodegradable elastomer are linear, constant, similar, and adjustable. Pharm Res. 2006;23:782–9.
38. Hirose K, Marui A, Arai Y, Nomura T, Inoue S, Kaneda K, *et al.* Sustained-release vancomycin sheet may help to prevent prosthetic graft methicillin-resistant Staphylococcus aureus infection. J Vasc Surg. 2006;44:377–82.
39. Li B, Davidson JM, Guelcher SA. The effect of the local delivery of platelet-derived growth factor from reactive two-component polyurethane scaffolds on the healing in rat skin excisional wounds. Biomaterials. 2009;30:3486–94.
40. Cui F, Cun D, Tao A, Yang M, Shi K, Zhao M, *et al.* Preparation and characterization of melittin-loaded poly (dl-lactic acid) or poly (dl-lactic-co-glycolic acid) microspheres made by the double emulsion method. J Control Release. 2005;107:310–9.
41. Lin CC, Metters AT. Hydrogels in controlled release formulations: network design and mathematical modeling. Adv Drug Deliv Rev. 2006;58:1379–408.
42. Cometa S, Bartolozzi I, Corti A, Chiellini F, De Giglio E, Chiellini E. Hydrolytic and microbial degradation of multi-block polyurethanes based on poly([var epsilon]-caprolactone)/poly (ethylene glycol) segments. Polym Degrad Stab. 2010;95:2013–21.
43. Santerre JP, Woodhouse K, Laroche G, Labow RS. Understanding the biodegradation of polyurethanes: from classical implants to tissue engineering materials. Biomaterials. 2005;26:7457–70.
44. Labow RS, Meek E, Santerre JP. Hydrolytic degradation of poly (carbonate)-urethanes by monocyte-derived macrophages. Biomaterials. 2001;22:3025–33.
45. Labow RS, Meek E, Santerre JP. Model systems to assess the destructive potential of human neutrophils and monocyte-derived macrophages during the acute and chronic phases of inflammation. J Biomed Mater Res. 2001;54:189–97.
46. Peng H, Ling J, Liu J, Zhu N, Ni X, Shen Z. Controlled enzymatic degradation of poly(caprolactone)-based copolymers in the presence of porcine pancreatic lipase. Polym Degrad Stab. 2010;95:643–50.
47. Labow RS, Erfle DJ, Santerre JP. Neutrophil-mediated degradation of segmented polyurethanes. Biomaterials. 1995;16:51–9.
48. Labow RS, Sa D, Matheson LA, Dinnes DLM, Paul Santerre J. The human macrophage response during differentiation and biodegradation on polycarbonate-based polyurethanes: dependence on hard segment chemistry. Biomaterials. 2005;26:7357–66.
49. Tang YW, Labow RS, Revenko I, Santerre JP. Influence of surface morphology and chemistry on the enzyme catalyzed biodegradation of polycarbonate-urethanes. J Biomater Sci Polym Ed. 2002;13:463–83.
50. Pérez C, Castellanos IJ, Costantino HR, Al-Azzam W, Griebenow K. Recent trends in stabilizing protein structure upon encapsulation and release from bioerodible polymers. J Pharm Pharmacol. 2002;54:301–13.
51. Davis ME, Hsieh PC, Takahashi T, Song Q, Zhang S, Kamm RD, *et al.* Local myocardial insulin-like growth factor 1 (IGF-1) delivery with biotinylated peptide nanofibers improves cell therapy for myocardial infarction. Proc Natl Acad Sci USA. 2006;103:8155–60.
52. Carrascosa C, Torres-Aleman I, Lopez-Lopez C, Carro E, Espejo L, Torrado S, *et al.* Microspheres containing insulin-like growth factor I for treatment of chronic neurodegeneration. Biomaterials. 2004;25:707–14.
53. Lam XM, Duenas ET, Daugherty AL, Levin N, Cleland JL. Sustained release of recombinant human insulin-like growth factor-I for treatment of diabetes. J Control Release. 2000;67:281–92.
54. Tambara K, Premaratne GU, Sakaguchi G, Kanemitsu N, Lin X, Nakajima H, *et al.* Administration of control-released hepatocyte growth factor enhances the efficacy of skeletal myoblast transplantation in rat infarcted hearts by greatly increasing both quantity and quality of the graft. Circulation. 2005;112:I129–34.